ELSEVIER

Journal of Nuclear Materials 297 (2001) 327–331

journal of nuclear materials

www.elsevier.com/locate/jnucmat

Effect of a trivalent dopant, Gd^{3+}, on the oxidation of uranium dioxide

Jong-Goo Kim *, Yeong-Keong Ha, Soon-Dal Park, Kwang-Yong Jee, Won-Ho Kim

Nuclear Chemistry Research Team, Korea Atomic Energy Research Institute, P.O. Box 105, Yusong, Taejon 305-600, Republic of Korea

Received 19 July 2000; accepted 21 May 2001

Abstract

The effect of a trivalent dopant, Gd^{3+}, on the oxidation of doped UO_2 was investigated using thermogravimetry and X-ray diffraction (XRD) analysis. Gd-doped stoichiometric UO_2's of various dopant contents [$y = 0$–0.29 in $(U_{1-y}Gd_y)O_2$] were prepared. Weight gains by oxygen with increasing temperature for pulverized specimens were measured to obtain the oxidation kinetic curves. The oxidation kinetic curve for undoped UO_2 shows a two-step reaction: $UO_2 \rightarrow U_4O_9$ in the first step and $U_4O_9 \rightarrow U_3O_8$ in the second step. Decrease of the gradients of the oxidation kinetic curves for the first step with increasing content of Gd suggests that Gd dopant slowed down the reaction from $(U_{1-y}Gd_y)O_2$ to $(U_{1-y}Gd_y)_4O_9$. Calculated O/(U + Gd) values from the weight gains and the deflection patterns of final stage of the oxidation revealed that the degree of oxidation from $(U_{1-y}Gd_y)O_2$ to $(U_{1-y}Gd_y)_3O_8$ decreased linearly with increasing content of Gd. Such behavior as the slowdown and the inhibition were interpreted by the chemical states of U atoms in the lattice structures depending on doping of Gd^{3+}.

PACS: 28.41.Kw

1. Introduction

When exposed to an oxidizing atmosphere, UO_2 oxidizes readily to U_3O_8 accompanied by phase transformation from cubic fluorite to orthorhombic and by a 36% volume expansion, which has been considered to be a reason of spent fuel rupture during dry storage condition. Thus, numerous studies on the oxidation behavior of irradiated UO_2 fuel have been carried out by AECL [1–7] and PNL [8–12].

McEachern and Taylor [13] reviewed several parameters such as temperature, moisture, dopants, etc. which could affect the rate of UO_2 oxidation. In the review, an attention was paid to the enhanced stability of doped UO_2 and U_4O_9 resulting in the retention of cubic phases to higher temperatures compared with pure UO_2. However, more precise theoretical understanding to explain the enhanced stability of cubic phases of doped uranium oxides has not yet been achieved.

During irradiation, a large number of fission products are generated with typical yields. Among them, Sr, Zr, Nb and rare earth elements (REEs) are known to be dissolved as a solid solution in UO_2 matrices [14]. Gd has often been chosen as a dopant in simulated spent fuels [8,11,15] because it has been proposed as a burnable absorber for the urania–gadolinia fuels modified to extend cycle length [16].

In the present work, the oxidation kinetic curves of Gd-doped stoichiometric UO_2 in air were obtained in the temperature increasing from 50°C to 540°C. Quantitative effect of the dopant on the reaction $(U_{1-y}Gd_y)O_2 \rightarrow (U_{1-y}Gd_y)_3O_8$ are interpreted in terms of formal charges of uranium atoms affected by the content of Gd.

* Corresponding author. Tel.: +82-42 868 2483; fax: +82-42 868 8148.

E-mail address: njgkim@kaeri.re.kr (J.-G. Kim).

0022-3115/01/$ - see front matter
PII: S0022-3115(01)00639-0

2. Experimental

2.1. Preparation of Gd-doped stoichiometric UO_2

U_3O_8 and Gd_2O_3 were of reagent grade and used as starting materials without further purification. The content of U in U_3O_8 was determined by the Davis & Grey potentiometric titration method. The purity of Gd_2O_3 was >99.999% claimed by the supplier (Aldrich). Calculated amounts of U_3O_8 and Gd_2O_3 were ground and blended thoroughly using an agate mortar in a glove box to give a certain composition of $(U_{1-y}Gd_y)O_{2.00}$ where y ranged from 0 to 0.29. The y values of each $(U_{1-y}Gd_y)O_{2.00}$ are shown in Table 1. Sintered pellets were prepared by compacting the powders followed by sintering in hydrogen atmosphere at 1700°C for 4 h and annealing in the same atmosphere at 1200°C for 12 h. To make the O/M ratio be stoichiometric, the sintered pellets were further heated at 800°C over 24 h under the specific atmosphere of $CO/CO_2 = 10$ [17]. The pellets were finally pulverized in an agate mortar for thermogravimetric measurements. Particle sizes of the specimen were observed to be in the range of 2–5 μm by scanning electron microscopy (SEM). X-ray diffraction (XRD) patterns were obtained in the range from 15° to 90° by Siemens D5000 diffractometer. The CuKα line was used and filtered through a Ni foil (beam current 40 mA at 40 kV).

2.2. Thermogravimetric measurements

The weight gains by oxygen were measured in continuous air flow at 1 atm. and temperatures ranging from 50°C to 540°C at a heating rate of 1°C/min using Setaram TGA-92 thermoanalyzer.

2.3. Batch oxidation and phase characterization

The same pulverized specimens as used for the thermogravimetric measurements were heated under air atmosphere for 1 h at 420°C. This temperature was chosen from the second stage in the thermogravimeric curves (afterward called the oxidation kinetic curves), where no further weight gains by oxygen occurred. After cooling, powder XRD measurements were carried out with a scanning step of 0.02° for 10 s at each count in order to identify their structural change.

Table 1
O/(U + Gd) ratios and calculated composition of $(U_{1-y}Gd_y)_4O_9$ and $(U_{1-y}Gd_y)_3O_8$ at the final stage in oxidation

Gd content (y)	O/(U + Gd) ratios	Fraction	
		$(U_{1-y}Gd_y)_4O_9$	$(U_{1-y}Gd_y)_3O_8$
Undoped	2.68	0.000	1.000
0.025	2.66	0.017	0.983
0.049	2.62	0.113	0.887
0.071	2.55	0.281	0.719
0.092	2.53	0.329	0.671
0.132	2.51	0.376	0.624
0.169	2.46	0.496	0.504
0.234	2.38	0.688	0.312
0.289	2.31	0.856	0.144

3. Results and discussion

3.1. Characterization of specimens

The lattice parameter, a (pm) of the specimens decreased linearly with increasing Gd content [y values in $(U_{1-y}Gd_y)O_2$] as shown in Fig. 1. Applying Vegard's law [18] to the results, this linear relationship indicates that the specimens were of the same solid solution and their structure remained as a fluorite structure of UO_2 in the given range ($y = 0$–0.29) of Gd content.

3.2. Analysis of thermogravimetric measurements

Oxidation kinetic curves were obtained as the gradient of weight gains by oxygen against increasing temperature. The weight gains by oxygen, G_O, is expressed as Eq. (1),

$$G_O = (W_1 - W_2)/W_2, \tag{1}$$

where W_1 is the weight of the specimen at a certain temperature during oxidation, and W_2 is the weight of stoichiometric specimen before oxidation. Eq. (1) can be converted to the O/(U + Gd) ratio by Eq. (2)

$$O/(U + Gd) = 2 + G_O(W_M/16), \tag{2}$$

where W_M is molecular weight of the stoichiometric specimen.

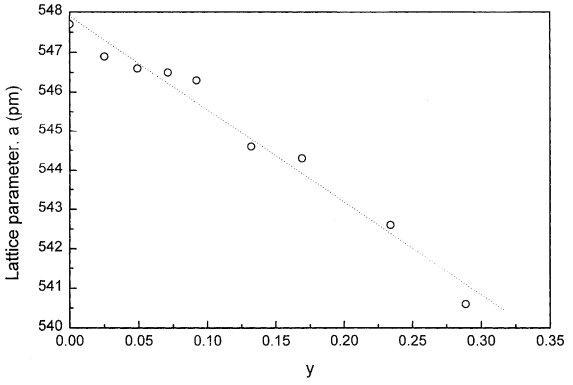

Fig. 1. Lattice parameter of $(U_{1-y}Gd_y)O_{2.00}$ versus Gd content (y) in $(U_{1-y}Gd_y)O_{2.00}$ at a room temperature.

The O/(U + Gd) ratio has a linear relationship with the weight gain by oxygen and gives more useful information about the characteristics of the phases. Thus the weight gains in the oxidation kinetic curves can be replaced by the corresponding O/(U + Gd) ratios and the result is shown in Fig. 2, which is normally the same as the one with the weight gains.

The curve from undoped UO_2 in Fig. 2 shows the typical two-step process in the oxidation reaction [17]: the one, from the temperature near 150°C, where the weight gain by oxygen starts, to the first plateau (290–310°C), and the other, from this plateau to the next plateau, where the O/U ratio remains constant. The value of O/U ratio 2.25 at the first plateau corresponds exactly to U_4O_9 and the value 2.67 at the second plateau comes from U_3O_8. This indicated that the oxidation of undoped UO_2 proceeded as a sequential process, which is to say, UO_2 oxidized to U_4O_9 in the first step and continued further oxidation to U_3O_8 in the second step. Comparing this oxidation kinetic curve with those from the doped specimens, distinction between the two steps of the curves became less pronounced as the content of Gd increased. Moreover, the O/(U + Gd) ratios at the first plateau gradually decreased from the value 2.25 as the content of Gd increased. The oxidation of Gd-doped UO_2 did not clearly proceed through two steps, quite unlike that of undoped UO_2. Changes in the reaction kinetics can be related to the changes in the slopes of the oxidation kinetics curves. The gradients of the oxidation kinetics curves for the first step decreased as the content of Gd increased. Also, those for the second step decreased, however, the decrease was not as apparent as for the first step. This means that Gd dopant can slow down the initial oxidation kinetics from $(U_{1-y}Gd_y)O_2$ to $(U_{1-y}Gd_y)_4O_9$. The O/(U + Gd) ratios in the final stage of the reactions decreasing gradually with Gd content indicated that Gd inhibited the reaction corresponding to the second step of the oxidation.

The batch oxidation and XRD analysis described in Section 2.3 were performed to get information on the phases in the final stage. As shown in Fig. 3, two types of diffraction patterns were observed corresponding to the phases of U_4O_9 and U_3O_8. Therefore, it can be deduced that two phases of $(U_{1-y}Gd_y)_4O_9$ and $(U_{1-y}Gd_y)_3O_8$ coexist at the final stage of oxidation. This information permits the calculation of the composition of the phases by O/(U + Gd) ratios and Eq. (3)

$$O/(U + Gd) = (9/4)X + (8/3)Y, \quad (3)$$

where X and Y are the composition of each phases, $(U_{1-y}Gd_y)_4O_9$ and $(U_{1-y}Gd_y)_3O_8$, respectively, and their sum is equal to 1. Calculated values of the compositions of two phases are listed in Table 1. The composition of $(U_{1-y}Gd_y)_3O_8$ decreased with increasing content of Gd dopant while that of $(U_{1-y}Gd_y)_4O_9$ increased. To determine the relationship between the compositions and Gd content, the fractions of $(U_{1-y}Gd_y)_3O_8$ were plotted

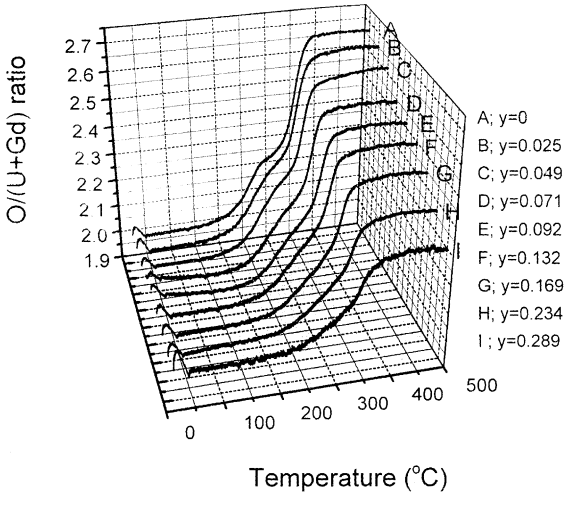

Fig. 2. Oxidation kinetic curves for the oxidation of powdered $(U_{1-y}Gd_y)O_{2.00}$.

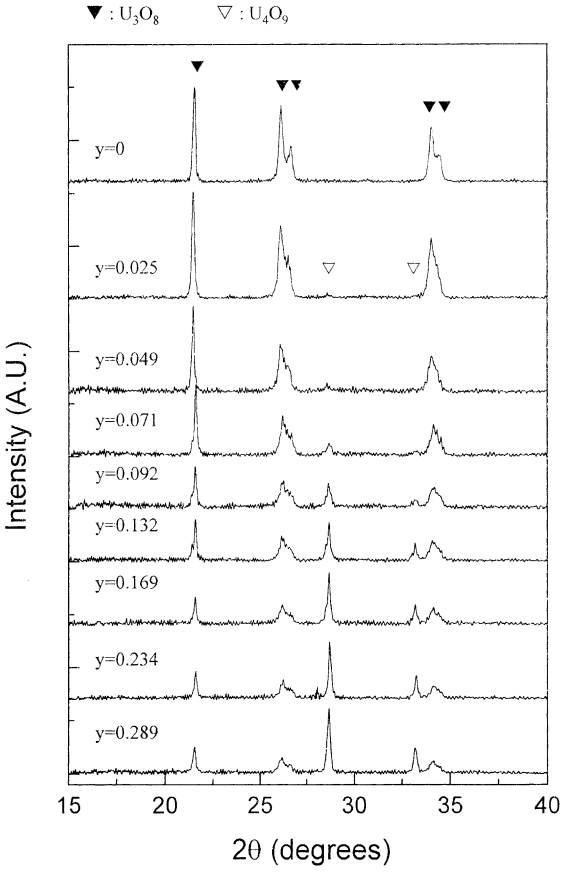

Fig. 3. XRD patterns for the final stage of oxidation of $(U_{1-y}Gd_y)O_{2.00}$.

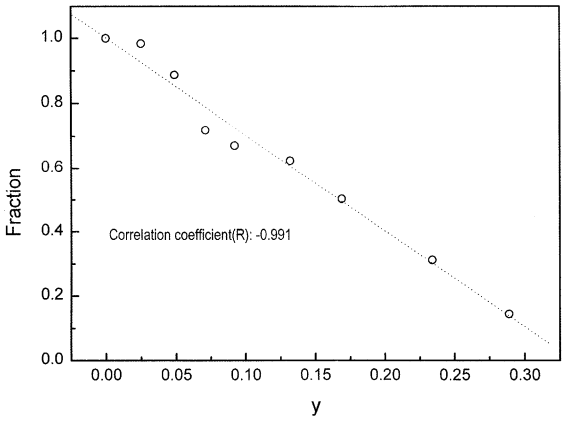

Fig. 4. Composition of $(U_{1-y}Gd_y)_3O_8$ versus Gd content (y) at 420°C in the final stage of oxidation of $(U_{1-y}Gd_y)O_{2.00}$.

against the contents (y) of Gd, as shown in Fig. 4. The figure shows a linear relationship with a negative slope between them; the composition of $(U_{1-y}Gd_y)_3O_8$ formed decreased linearly with Gd content. The figure also indicates that complete oxidation to $(U_{1-y}Gd_y)_3O_8$ is prevented by the Gd dopant.

The oxidation reaction kinetics from $(U_{1-y}Gd_y)O_2$ to $(U_{1-y}Gd_y)_4O_9$ and the extent of inhibition in the oxidation reaction of $(U_{1-y}Gd_y)_4O_9$ to $(U_{1-y}Gd_y)_3O_8$ were found to be closely related with the content of Gd. To interpret this behavior, it is necessary to consider the Gd dopant effect on the chemical states of U atoms, i.e., the charge of U atoms in each phase. As the oxidation of UO_2 to U_3O_8 is accompanied by the increase of charge of U atoms, the change of the charge of U atoms by the dopant could influence the oxidation reaction, either kinetically or thermodynamically.

3.3. Chemical states of U atoms in the oxide phases

The effective nuclear charge of an atom could be considered as the real chemical state of the atom, however, it is not easy to get a true value. Instead, the formal charge can usually be used as a matter of convenience. The chemical state of U atoms in cubic fluorite structure of UO_2 is generally regarded as to be U^{4+} against O^{2-}. In case of REE^{3+}-doped UO_2, however, some portion of U atoms in the lattice would exist with higher charges such as U^{5+} or U^{6+} because of a charge compensation for the lower charge of REE^{3+} introduced in the doped UO_2. It is not clearly confirmed which is the correct oxidation state, U^{5+} or U^{6+}, in REE^{3+}-doped UO_2. However, U^{5+} was used in recent modeling studies for the prediction of thermodynamic values; e.g., the oxygen potentials of doped UO_2 on the basis of defect structures such as UO_{2+x} [19–21], or the interpretation of the lattice parameter depending on the dopant content using a simple ionic model [22–24]. Recently, it was reported that U^{4+} and U^{6+} could coexist as U_4O_9, U_3O_7 and U_3O_8 in studies for identification of the chemical states for U atoms in several undoped uranium oxide phases by XPS [2,3,25].

3.4. Effect of Gd^{3+} on the chemical state and the oxidation reaction

In the oxidation reaction from UO_2 to U_4O_9, extra oxygen atoms from the outside occupy interstitial sites of the UO_2 lattice as an oxide, O^{2-}, accompanying the oxidation of U^{4+} to U^{6+} to maintain electrical neutrality. In the case of Gd-doped UO_2, the doping of Gd^{3+} on U^{4+} sites in the fluorite lattice would lead to a coexistence of U^{4+} and U^{5+}, such as $[U^{4+}_{1-2y}U^{5+}_yGd^{3+}_yO^{2-}_2]_{\text{fluorite}}$, as discussed in Section 3.3. Therefore, the composition of U^{4+} and U^{5+} should be a function of Gd content. Their calculated values of the composition are listed in Table 2, considering the formal charge balance of $[U^{4+}_{1-2y}U^{5+}_yGd^{3+}_yO^{2-}_2]$ and the content of Gd. The higher the content of Gd, y, is, the lower the content of U^{4+}, $1-2y$, is.

By increasing Gd content in UO_2, the decrease of U^{4+} should result in lowering the gradient of the oxidation kinetic curves (Section 3.2). This means that the reaction rate of the first oxidation step depends on the Gd content. The content of U^{4+} rather than U^{5+} in $[U^{4+}_{1-2y}U^{5+}_yGd^{3+}_yO^{2-}_2]_{\text{fluorite}}$ should be a main factor controlling the rate in the oxidation reaction of Gd-doped UO_2, especially in the first step, from $(U_{1-y}Gd_y)O_2$ to $(U_{1-y}Gd_y)_4O_9$.

The accurate chemical states of U atoms in the oxide phases such as $(U_{1-y}Gd_y)_4O_9$ and $(U_{1-y}Gd_y)_3O_8$ are unknown. The mean formal charge of the U atoms in the final stage of oxidation can be calculated from the Gd content with the chemical formula of each oxide phase, as listed in Table 3. Finally, the relationship between the mean formal charge and the composition in a mixture at the end of reaction, such that the sum of their products is a constant value of 5.3, can be established as follows:

Table 2
Calculated composition of U^{4+} and U^{5+} in $[U^{4+}_{1-2y}U^{5+}_yGd^{3+}_yO^{2-}_2]_{\text{fluorite}}$

Gd content (y)	U^{4+} $(1-2y)$	U^{5+} (y)
Undoped	1	0
0.025	0.95	0.025
0.049	0.90	0.049
0.071	0.86	0.071
0.092	0.82	0.092
0.132	0.74	0.132
0.169	0.66	0.169
0.234	0.53	0.234
0.289	0.42	0.289

Table 3
Calculated mean formal charges on U in $(U_{1-y}Gd_y)_4O_9$, $(U_{1-y}Gd_y)_3O_8$ and measured average formal charge on U at the final stage of the reaction

Gd content, (y)	Mean formal charge on U		Composition at the final stage		Measured average formal charge[a]
	(4,9)[b]	(3,8)[b]	(4,9)[b]	(3,8)[b]	
Undoped	4.5	5.33	0.000	1.000	5.33
0.025	4.54	5.39	0.017	0.983	5.38
0.049	4.58	5.45	0.113	0.887	5.35
0.071	4.61	5.51	0.281	0.719	5.26
0.092	4.65	5.57	0.329	0.671	5.27
0.132	4.73	5.69	0.376	0.624	5.33
0.169	4.81	5.81	0.496	0.504	5.31
0.234	4.96	6.05	0.688	0.312	5.30
0.289	5.11	6.28	0.856	0.144	5.28

[a] $\sum(\text{mean formal charge} \times \text{composition})_{\text{final state}}$.
[b] $(4,9) \rightarrow (U_{1-y}Gd_y)_4O_9$; $(3,8) \rightarrow (U_{1-y}Gd_y)_3O_8$.

$$\sum(\text{mean formal charge} \times \text{compostion})_{\text{final state}} \cong 5.3.$$

This means that the oxidation of $(U_{1-y}Gd_y)_4O_9$ to $(U_{1-y}Gd_y)_3O_8$ proceeds within a certain limit, that is, the oxidation to $(U_{1-y}Gd_y)_3O_8$ is strongly inhibited when the average formal charge of U atoms in the oxidation products reaches a value of 5.3.

4. Conclusions

In the oxidation reaction of $(U_{1-y}Gd_y)O_2$ to $(U_{1-y}Gd_y)_3O_8$, the slowdown due to Gd as a dopant occurs mainly in the first step, $(U_{1-y}Gd_y)O_2 \rightarrow (U_{1-y}Gd_y)_4O_9$. The decrease of U^{4+} content with increasing Gd content seems to be a main factor causing such slowdown. The degree of oxidation to $(U_{1-y}Gd_y)_3O_8$ phase from $(U_{1-y}Gd_y)O_2$ can be quantitatively correlated with the formal charge on U atoms in the phases as determined by Gd content. The results are applicable to interpret the oxidation behavior of spent fuel containing various fission products.

Acknowledgements

We acknowledge that this project has been carried out under the Nuclear R&D Program by the Ministry of Science and Technology.

References

[1] P. Taylor, R.J. McEachern, D.C. Doern, D.D. Wood, J. Nucl. Mater. 256 (1998) 213.
[2] R.J. McEachern, S. Sunder, P. Taylor, D.C. Doern, N.H. Miller, D.D. Wood, J. Nucl. Mater. 255 (1998) 234.
[3] S. Sunder, N.H. Miller, J. Nucl. Mater. 231 (1996) 121.
[4] J.-W. Choi, R.J. McEachen, P. Taylor, D.D. Wood, J. Nucl. Mater. 230 (1996) 250.
[5] K.M. Wasywich, W.H. Hocking, D.W. Shoesmith, P. Taylor, Nucl. Technol. 104 (1993) 309.
[6] P. Taylor, D.D. Wood, A.M. Duclo, J. Nucl. Mater. 189 (1992) 116.
[7] P. Taylor, D.D. Wood, A.M. Duclo, D.G. Owen, J. Nucl. Mater. 168 (1989) 70.
[8] L.E. Thomas, R.E. Einziger, H.C. Buchanan, J. Nucl. Mater. 201 (1993) 310.
[9] R.E. Einziger, L.E. Thomas, H.C. Buchanan, J. Nucl. Mater. 190 (1992) 53.
[10] R.E. Woodley, R.E. Einziger, H.C. Buchanan, Nucl. Technol. 85 (1989) 74.
[11] T.K. Campbell, E.R. Gibert, G.D. White, G.F. Piepel, B.J. Wrona, Nucl. Technol. 85 (1989) 160.
[12] T.K. Campbell, E.R. Gibert, C.K. Thornhill, B.J. Wrona, Nucl. Technol. 84 (1989) 182.
[13] R.J. McEachern, P. Taylor, J. Nucl. Mater. 254 (1998) 87.
[14] H. Kleykamp, Nucl. Technol. 80 (1988) 412.
[15] G.-S. You, K.-S. Kim, D.-K. Min, S.-G. Ro, J. Nucl. Mater. 277 (2000) 325.
[16] IAEA, International Atomic Energy Agency Report, IAEA-TECDOC-844.
[17] J. Cobos, D. Papaioannou, J. Spino, M. Coquerelle, J. Alloys Compounds 271–273 (1998) 610.
[18] A.R. West, in: Basic Solid State Chemistry, Wiley, New York, 1991, p. 253.
[19] K. Park, D.R. Olander, J. Nucl. Mater. 187 (1992) 89.
[20] T. Fujino, N. Sato, J. Nucl. Mater. 189 (1992) 103.
[21] H.S. Kim, Y.K. Yoon, Y.W. Lee, J. Nucl. Mater. 226 (1995) 206.
[22] S.K. Sali, S. Sampath, V. Venugopal, J. Nucl. Mater. 232 (1996) 23.
[23] T. Tsuji, M. Iwashita, T. Yamashita, K. Ohuchi, J. Alloys Compounds 271 (1998) 391.
[24] H.S. Kim, D.S. Sohn, J. Korean Nucl. Soc. 28 (1996) 118.
[25] S. Sunder, N.H. Miller, W.H. Hocking, J. Alloys Compounds 213&214 (1994) 503.